

Modelling of deuterium chemistry and its application to molecular clouds

H. Roberts and T.J. Millar

Department of Physics, UMIST, P.O. Box 88, Manchester M60 1QD, UK

Received 22 May 2000 / Accepted 4 July 2000

Abstract. We have developed new models of the chemistry of deuterium for investigating fractionation in interstellar molecular clouds. We have incorporated the latest information on reactions which affect deuteration, extended previous models to include S-D bonds for the first time and included the gas-phase chemistry of some doubly-deuterated species. We present models for a wide range of physical parameters, including density, temperature, elemental abundances, and the freeze out of molecules on to dust grains. We discuss the detailed fractionation of particular species and show how fractionation can be used to probe the history of interstellar matter. The freeze out of molecules onto dust leads to significant enhancement in fractionation ratios and, in particular, to large fractionation in doubly-deuterated species.

Key words: ISM: abundances – ISM: molecules – galaxies: abundances – galaxies: ISM – galaxies: Magellanic Clouds

1. Introduction

Observations of deuterium in interstellar molecules have long been used to probe the physical conditions within interstellar clouds, the detailed synthetic routes by which molecules form, the baryon density in the early universe, and the connection between interstellar and cometary ices. This wealth of information is valuable to us because the abundance of D atoms in molecules is much enhanced over the cosmic D/H abundance ratio, $\sim 1.5 \times 10^{-5}$, due to small zero-point energy differences which ensure that deuterium is preferentially bonded into molecules compared to hydrogen.

The usefulness of deuterium as a probe rests on our ability to understand the chemical kinetic processes by which it is incorporated into molecules. In this paper, we investigate the chemistry of deuterium over a much wider parameter space than heretofore and present results which can be applied to high and low temperature environments, and high and low metallicities. We have included the deuterium chemistry of sulphur for the first time and the gas-phase chemistry of some doubly-deuterated species. By investigating the enhancement of deuterium in molecules under conditions in which depletion of

molecules on to dust grains is operating, we show that a large abundance of D_2CO can arise without the need for any active surface chemistry.

In Sect. 2 we describe our approach to modelling. Sect. 3 shows how fractionation depends on physical parameters, such as temperature, density, and elemental abundances, using results from our gas-phase model, while Sect. 4 discusses the application of the models to observations involving sulphur-bearing species, doubly deuterated species, and deuterated molecules in continuum clumps. Throughout, we have adopted the conventions: '[ABC]' means the fractional abundance of molecule ABC; 'fractionation of XD' means $[XD]/[XH]$.

Many of our results are presented in the form of grid plots each of which summarizes the output of 100 time-dependent chemical kinetic models. In total, we have calculated over 300 independent models in the course of this study. Those interested in particular species and model results can contact the authors directly for further information.

2. The model

2.1. The gas-phase model

We are using a pseudo-time-dependent chemical model, which calculates the varying abundances of 285 species (122 of them containing deuterium) linked by 5260 reactions. The only grain-surface reactions included are for the formation of H_2 and HD. Our approach is based on that of Millar et al. (1989), hereafter MBH, but the reaction and species sets have been substantially extended and updated in the light of recent experimental and observational results and we have included a deuterated sulphur chemistry for the first time.

The reactions and rate coefficients for our basic reaction set are mostly taken from the UMIST database (Millar et al. 1997), but the species set has been extended to include mono-deuterated analogues of all hydrogen bearing species, as well as a small number of doubly deuterated species. In generating the deuterated reaction set we have adopted the approach described by MBH and Rodgers & Millar (1996). Thus, we assume that both deuterium- and hydrogen-bearing species react with the same species at the same rate. Where there is uncertainty into which product the deuterium atom is incorporated we assume statistical branching ratios between the various possibilities.

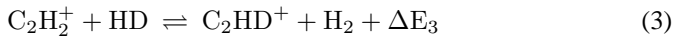
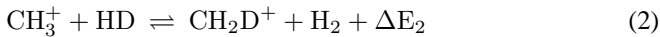
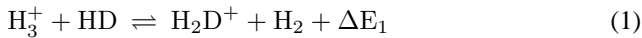
Send offprint requests to: H. Roberts (hr@janus4.phy.umist.ac.uk)

Of course, these assumptions can be questioned. For ion-neutral reactions, whose rate coefficients depend only the dipole moment and polarisability of the neutral, the rate coefficients should not vary by more than a few percent when a D is substituted for a H. However, a reaction which proceeds via quantum tunneling of hydrogen atoms will occur much more slowly when the heavier deuterium atoms are involved (Bell et al. 1988). Since this depends on a detailed understanding of the reaction process it is difficult to include in a large reaction scheme in any systematic way.

Where available, we have replaced reaction rate coefficients and statistically determined branching ratios with new results from experiments. For example, Larsson et al. (1996) measured the recombination rate coefficient for H_2D^+ and found that it was, in fact, a factor of two slower than the corresponding reaction for H_3^+ (determined by Sundström et al. 1994). They also determined the branching ratios for each possible product channel and found that, although the two-body/three-body branching ratio is the same as for H_3^+ , the products $\text{HD} + \text{H}$ are three times more likely than $\text{H}_2 + \text{D}$, not twice as likely as simple statistical arguments would suggest. We have also included theoretically determined rate coefficients for several radiative association reactions involving deuterated species, derived by MBH. As the reactions involving deuterated species proceed more quickly than their hydrogen analogues, these strongly affect the temperature dependence of fractionation, especially at early times.

In addition to deuterating the existing reactions in a particular set, it is necessary to include a number of direct fractionation reactions. These are listed in Table 1 along with their rate coefficients. The complete reaction set is available from the authors.

At low temperatures (< 100 K) the most important of the fractionation reactions are;



where $\Delta E_1 \sim 220$ K, falling to ~ 130 K for temperatures greater than 100 K, $\Delta E_2 \sim 370$ K and $\Delta E_3 \sim 550$ K.

The equilibrium fractionation of the species in reacs. (1)–(3) can be estimated by assuming that the rate coefficients for both directions are equal, except for a Boltzmann factor, $\exp\{-\Delta E/T\}$, in the reverse direction. Thus, the fractionation has an exponential dependence on $1/T$, though at very low temperatures, when the reactions become essentially irreversible, other destruction reactions for the deuterated ions become important. It is these destructions which propagate deuterium throughout the system and transfer the fractionation of the primary ions to other species. For H_2D^+ this can be described by the following equation;

$$\frac{[\text{H}_2\text{D}^+]}{[\text{H}_3^+]} = \frac{k_f}{k_f e^{-\Delta E/T} + k_e[e^-] + \sum k_i[M_i]} \frac{[\text{HD}]}{[\text{H}_2]} \quad (4)$$

where k_f is the rate coefficient for formation via reac. (1), k_e is the rate coefficient for dissociative recombination of H_2D^+ with

Table 1. Deuterium fractionation reactions

Reaction	α ($\text{cm}^3 \text{s}^{-1}$)	β	γ (K)
$\text{H}_3^+ + \text{HD} \rightarrow \text{H}_2\text{D}^+ + \text{H}_2$	1.7(-09)	-	1
$\text{H}_2\text{D}^+ + \text{H}_2 \rightarrow \text{H}_3^+ + \text{HD}$			1*
$\text{CH}_3^+ + \text{HD} \rightarrow \text{CH}_2\text{D}^+ + \text{H}_2$	1.3(-09)	-	2
$\text{CH}_2\text{D}^+ + \text{H}_2 \rightarrow \text{CH}_3^+ + \text{HD}$	8.7(-10)	-	370
$\text{C}_2\text{H}_2^+ + \text{HD} \rightarrow \text{C}_2\text{HD}^+ + \text{H}_2$	1.0(-09)	-	3
$\text{C}_2\text{HD}^+ + \text{H}_2 \rightarrow \text{C}_2\text{H}_2^+ + \text{HD}$	2.5(-09)	-	550
$\text{D}^+ + \text{H}_2 \rightarrow \text{H}^+ + \text{HD}$	2.1(-09)	-	2
$\text{H}^+ + \text{HD} \rightarrow \text{D}^+ + \text{H}_2$	1.0(-09)	-	464
$\text{D}^+ + \text{H} \rightarrow \text{H}^+ + \text{D}$	1.0(-09)	-	4
$\text{H}^+ + \text{D} \rightarrow \text{D}^+ + \text{H}$	1.0(-09)	-	41
$\text{H}_3^+ + \text{D} \rightarrow \text{H}_2\text{D}^+ + \text{H}$	1.0(-09)	-	5 [†]
$\text{H}_2\text{D}^+ + \text{H} \rightarrow \text{H}_3^+ + \text{D}$	1.0(-09)	-	632
$\text{HCO}^+ + \text{D} \rightarrow \text{DCO}^+ + \text{H}$	1.0(-09)	-	5
$\text{DCO}^+ + \text{H} \rightarrow \text{HCO}^+ + \text{D}$	2.2(-09)	-	796
$\text{N}_2\text{H}^+ + \text{D} \rightarrow \text{N}_2\text{D}^+ + \text{H}$	1.0(-09)	-	5
$\text{N}_2\text{D}^+ + \text{H} \rightarrow \text{N}_2\text{H}^+ + \text{D}$	2.2(-09)	-	550
$\text{OH} + \text{D} \rightarrow \text{OD} + \text{H}$	1.3(-10)	-	6
$\text{OD} + \text{H} \rightarrow \text{OH} + \text{D}$	1.3(-10)	-	810
$\text{C}_2\text{H} + \text{D} \rightarrow \text{C}_2\text{D} + \text{H}$	5.0(-11)	0.5	250
$\text{C}_2\text{D} + \text{H} \rightarrow \text{C}_2\text{H} + \text{D}$	5.0(-11)	0.5	832
$\text{HCN} + \text{D} \rightarrow \text{DCN} + \text{H}$	1.0(-10)	0.5	500
$\text{DCN} + \text{H} \rightarrow \text{HCN} + \text{D}$	1.0(-10)	0.5	500

* complicated temperature dependence, see text

[†] estimate

Notes: a(-b) stands for $a \times 10^{-b}$

The total rate coefficient; $k_r = \alpha (T/300)^\beta e^{(-\gamma/T)}$

References: 1: Sidhu et al. 1992; 2: Smith et al. 1982a,b; 3: Herbst et al. 1987; 4: Watson 1976; 5: Adams & Smith 1985; 6: Crosswell & Dalgarno 1985; 7: Schilke et al. 1992.

electrons and $[e^-]$ is the fractional abundance of electrons, while $\sum k_i[M_i]$ represents the destruction of H_2D^+ by other species like CO, H_2O and N_2 , $[M_i]$ being the fractional abundance of species i , and k_i the rate coefficient for its reaction with H_2D^+ . Similar equations can be written for CH_2D^+ and C_2HD^+ .

Each of the three terms in the denominator of Eq. (4) can be related to an important cloud parameter. The first term is simply dependent on temperature, so observations of species such as N_2D^+ , which is directly fractionated via deuteron transfer from H_2D^+ to N_2 , can give an upper limit to the temperature of the gas. The second and third terms give information about electron and elemental abundances respectively. The importance of these three parameters is discussed further in Sect. 3.

2.2. The depletion model

In cold, dense clouds gaseous species which collide with dust grains will tend to stick and so the grains begin to accrete icy mantles. This process occurs on a similar timescale to the physical and chemical evolution of these clouds and will strongly

affect their properties. For example, depletion of neutral species causes variations in the degree of ionisation, one of the fundamental parameters regulating the rate of star formation, while the disappearance of major gas coolants, such as CO, may affect the thermal balance of a dark cloud.

This is a growing area of research, since submillimetre bolometer cameras, such as SCUBA and SHARC, are now able to detect and map dust emission in molecular clouds and so identify likely candidates in which to search for molecular depletions.

As a first step towards incorporating grain-surface chemistry into our model we consider how the removal of species from the gas phase will affect the chemistry, and, in particular, the molecular D/H ratios, of our system.

As mentioned above, fractionation in cold clouds primarily stems from the enhancement of the $[\text{H}_2\text{D}^+]/[\text{H}_3^+]$ ratio, and the subsequent destruction of these ions by atoms and molecules such as CO, N_2 , O, C and H_2O . The major formation for H_2D^+ is through reac. (1), though in undepleted gas this represents a minor loss for H_3^+ . Once the other molecules begin to deplete from the gas, however, reaction with HD becomes the dominant loss mechanism for H_3^+ , producing H_2D^+ in the process. The result is that the $[\text{H}_2\text{D}^+]/[\text{H}_3^+]$ ratio increases as depletion sets in and that this enhancement results in an increase in molecular D/H ratios for the period before all heavy species freeze out.

We have extended the gas-phase model, described above, to include depletion onto grains. For most species reaction with a grain is treated as a destruction, as here we are only interested in how depletion is affecting the gas-phase abundances. We assume the rate coefficient for the reaction of each species with the grains to be;

$$k_{freeze} = S_x C_x < \pi a^2 n_g > v_x \quad (5)$$

(Willacy & Millar 1998). where S_x is the sticking coefficient (for which we adopt a value of 0.3), C_x is a factor which increases the freeze out rate of positively charged ions by the (assumed) negatively charged grains, a is the grain radius, n_g is the grain number density and v_x is the velocity of the particles. The exceptions are H^+ , D^+ , H_2^+ , HD^+ , H_3^+ , H_2D^+ and He, which are assumed not to stick, and He^+ , which is neutralized on collision with a grain and returned to the gas.

2.3. Model calculations

Unless otherwise stated, both our gas-phase and depletion models use the initial elemental abundances listed in Table 2. We have adopted the cosmic D/H ratio measured by Linsky et al. (1995), a cosmic ray ionisation rate of $1.3 \times 10^{-17} \text{ s}^{-1}$ and a visual extinction of 10 mags. We have investigated the effect of varying the C/O ratio between 0.3 and 0.5, but as the results presented here are largely independent of this parameter all our models use a constant ratio of ~ 0.4 .

It is generally expected that the molecular D/H ratios will be less sensitive to any variations in the physical parameters of a system than will the absolute abundances. This is because, even though the fractional abundances may change by orders

Table 2. The initial abundances used by our models.

Species	Initial Abundance (relative to H nuclei)
H_2	5.00×10^{-1}
He	1.40×10^{-1}
C^+	7.30×10^{-5}
N	2.14×10^{-5}
O	1.76×10^{-4}
H_3^+	1.00×10^{-11}
Si	2.00×10^{-8}
Fe^+	1.00×10^{-8}
S	1.00×10^{-7}
HD	1.60×10^{-5}

of magnitude, both the hydrogenated and deuterated forms of a particular species react in similar ways, leaving the ratio of their abundances unchanged.

However, deuterated species have now been observed in many different astrophysical environments where the variation in physical conditions or evolutionary history could well be affecting deuterium abundance. For example, in regions which have been less chemically processed than our local ISM, such as the Magellanic Clouds, we might expect to see evidence of a higher underlying D/H ratio, while towards the Galactic Centre the high rate of star formation should have destroyed most of the primordial deuterium. Even in more local regions there are still uncertainties – fractionation of deuterium-bearing species appears to be markedly different in low-mass star forming regions compared to their high-mass counterparts and we consider why this might be.

As a result, one of the aims of this paper is to explore a much larger parameter space than has been considered before. To illustrate the relative importance of various parameters we have made grid plots for particular molecules, each point on the grid being the fractionation of that molecule from a gas-phase model run with one set of physical parameters. These sort of plots are only really useful at steady-state because changing physical conditions may simply be changing the time scales for formation of molecules, thus a snapshot at early times may be misleading. In fact, grid plots made at early times generally show that, although the value of each point may have changed, the shape of the grid is the same.

For our depletion model, however, we cannot ignore the time-dependence of the ratios, as depletion occurs on a similar time scale to chemical evolution. This is illustrated in Fig. 1, which shows how the evolution of selected species differs from the purely gas-phase model. It also shows the expected increase in $[\text{DCO}^+]$, relative to $[\text{HCO}^+]$, as depletion sets in.

3. Results

In order to ensure that our deuterium chemistry is appropriate we have modeled the Taurus Molecular Cloud (TMC-1), one of the most studied dark clouds in our local ISM. Table 3 compares the molecular D/H ratios observed towards TMC-1 with the results

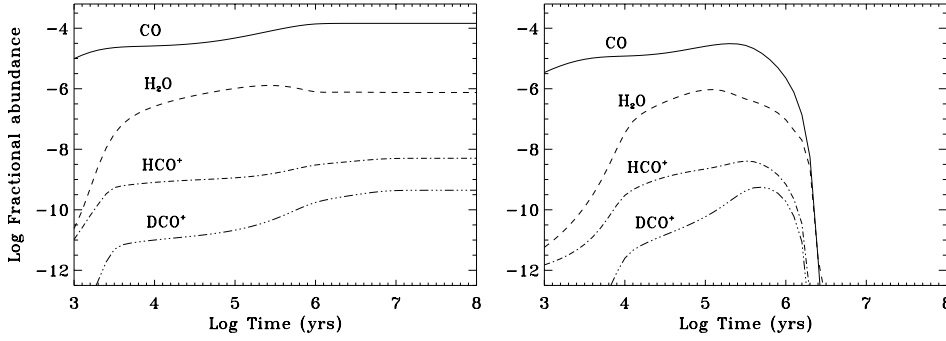


Fig. 1. A comparison of the fractional abundances of selected oxygen-bearing species predicted by our gas-phase (left) and depletion (right) models. $T_{\text{kin}} = 10$ K, $n(\text{H}_2) = 10^4 \text{ cm}^{-3}$.

Table 3. Comparison of molecular D/H ratios in TMC-1 with theoretical values at 10 K, $n(\text{H}_2) = 10^4 \text{ cm}^{-3}$. The bold values indicate good agreement (i.e. to within a factor of two) between modeled and observed ratios.

Species	Observed X[D]/X[H]	Modeled X[D]/X[H] after 10^5 yrs	steady state	Refs.
NH ₂ D	0.009–0.014	0.084	0.028	1
HDCO	0.005–0.11	0.042	0.055	2
DCN	0.023	0.009	0.025	3
DNC	0.015	0.015	0.015	2
C ₂ D	0.01	0.011	0.027	4
C ₄ D	0.004	0.004	0.029	5
DCO ⁺	0.02	0.019	0.087	1
N ₂ D ⁺	0.08	0.025	0.052	1
C ₃ HD	0.08–0.16	0.006	0.020	6
C ₃ H ₃ D	0.054–0.065	0.083	0.099	7
DC ₃ N	0.03–0.1	0.007	0.026	8
DC ₅ N	0.013	0.023	0.026	9
HDCS	0.02	0.040	0.046	10

References: 1: Tiné et al. 2000; 2: Guélin et al. 1982; 3: Wootten 1987; 4: Millar et al. 1989; 5: Turner 1989; 6: Bell et al. 1988; 7: Gerin et al. 1992; 8: Howe et al. 1994; 9: Macleod et al. 1981; 10: Minowa et al. 1997.

from our gas-phase model. Although some observed ratios are uncertain, because of large optical depths or self-absorption in the non-deuterated species, the agreement between calculated and observed values is encouraging.

One notable exception is the $[\text{C}_3\text{HD}]/[\text{C}_3\text{H}_2]$ ratio, which has been observed to be much higher than the models lead us to expect. This problem was noted by MBH, they suggested that, following the suggestion of Bell et al. (1988), as these molecules are primarily formed via dissociative recombination, the enhanced ratio may be due preferential ejection of H atoms. However, if this were the case then we might also expect to see a much higher $[\text{C}_2\text{D}]/[\text{C}_2\text{H}]$ ratio than has been observed, as these species are also products of dissociative recombination.

3.1. Dependence on temperature and density

The $[\text{H}_2\text{D}^+]/[\text{H}_3^+]$, $[\text{CH}_2\text{D}^+]/[\text{CH}_3^+]$ and $[\text{C}_2\text{HD}^+]/[\text{C}_2\text{H}_2^+]$ ratios are all enhanced at low temperatures, however the fact that H_3^+ is one of the most abundant molecular ions, coupled with

the fact that CH_3^+ and C_2H_2^+ undergo radiative association with the very abundant H_2 , mean that, below 25 K, it is H_2D^+ which is responsible for fractionating most other molecules in the system. Above 25 K, however, H_2D^+ is rapidly destroyed by H_2 , so between 30 and 80 K it is CH_2D^+ and C_2HD^+ which propagate deuterium.

Fig. 2 shows the first of our grid plots, illustrating how the steady-state fractionation of a few species, namely atomic deuterium (D), deuterated formaldehyde (HDCO) and deuterated ethanyl (C_2D), varies between 10 and 100 K for H_2 densities between 3×10^3 and 10^8 cm^{-3} .

As there is little enhancement of the $[\text{D}]/[\text{H}]$ ratio above 30 K we can deduce that the fractionation of atomic deuterium is controlled by that of H_2D^+ . In fact, atomic deuterium is primarily produced via the reaction chain;



Similarly, the $[\text{HDCO}]/[\text{H}_2\text{CO}]$ and $[\text{C}_2\text{D}]/[\text{C}_2\text{H}]$ ratios reflect the ratios of their precursor ions ($[\text{CH}_2\text{D}^+]/[\text{CH}_3^+]$ and $[\text{C}_2\text{HD}^+]/[\text{C}_2\text{H}_2^+]$, respectively), having peaks at around 50–60 K. The detailed mechanisms of this propagation of deuterium, and its time-dependence, have been discussed by MBH.

As the density increases the relative abundances of the ions and electrons will tend to fall. This is because the ion-molecule reactions which are destroying them become more important relative to the cosmic-ray ionisation reactions forming them. Thus, the abundances of atomic hydrogen and deuterium, which are primarily formed via dissociative recombination of molecular ions with electrons, will also fall, so the fact that the $[\text{D}]/[\text{H}]$ ratio increases slightly with density (shown in Fig. 2a) implies that $[\text{D}]$ is falling more slowly than $[\text{H}]$. The reason for this is that, although the abundance of H_3^+ is falling, the lowered $[e^-]$ means less of it is dissociated and more can react with HD to form H_2D^+ . In the same way, less H_2D^+ is dissociated so the fractionation of species formed via reaction of H_2D^+ is increased. This effect is not apparent in Figs. 2b and c. The precursor ions CH_3^+ and C_2H_2^+ undergo rapid radiative association with H_2 and it is the rates of these reactions, rather than dissociative recombination, which are the limiting factors in how much of these ions can react with HD.

Thus, for species fractionated via H_2D^+ , one expects molecular D/H ratios will tend to increase with increasing density. However, there may be other ways of fractionating species

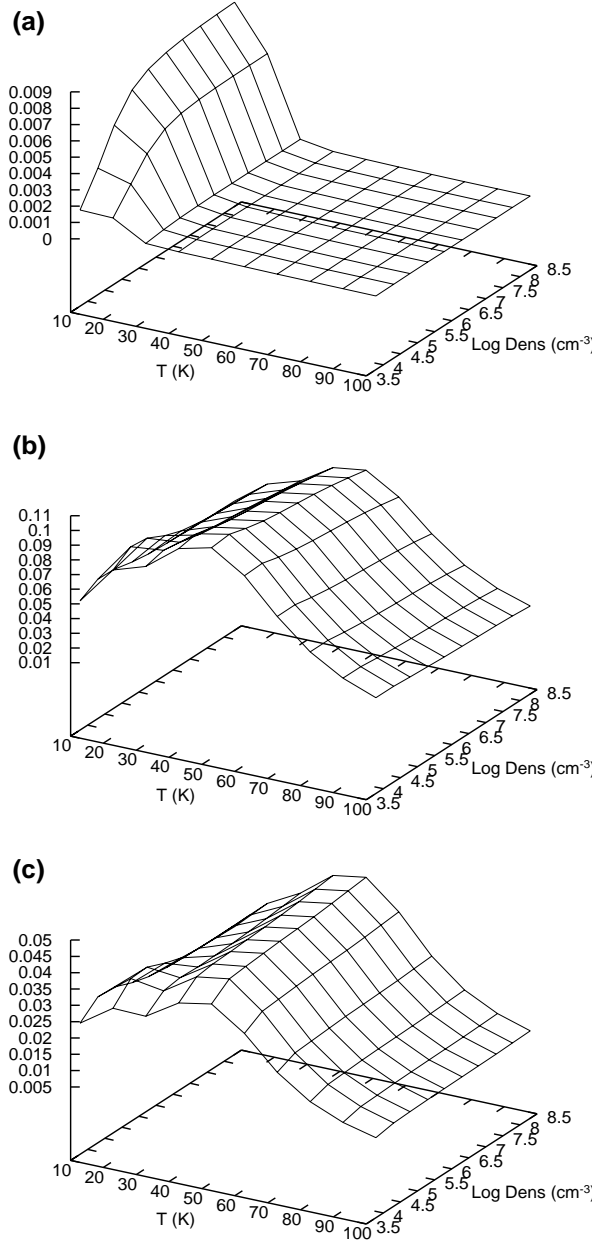
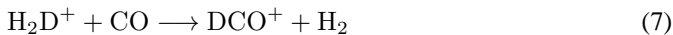


Fig. 2a–c. Steady-state molecular D/H ratios, from our gas-phase model, varying over a temperature range 10–100 K (in intervals of 10 K) and a $\log_{10}n(\text{H}_2)$ range of ~ 3.5 –8 (in intervals of 0.5); **a** $[\text{D}]/[\text{H}]$; **b** $[\text{HDCO}]/[\text{H}_2\text{CO}]$; **c** $[\text{C}_2\text{D}]/[\text{C}_2\text{H}]$.

which we have not taken into account. For example, at low temperatures, DCO^+ is primarily formed via the reaction;



where the statistical branching we have assumed should give a steady-state $[\text{DCO}^+]/[\text{HCO}^+]$ ratio approximately one-third of $[\text{H}_2\text{D}^+]/[\text{H}_3^+]$. This is true at higher densities (for $n(\text{H}_2)=10^6 \text{ cm}^{-3}$ at 10 K; $[\text{H}_2\text{D}^+]/[\text{H}_3^+] = 0.13$ and $[\text{DCO}^+]/[\text{HCO}^+] = 0.04$), but, as Fig. 3 shows, below 30 K there

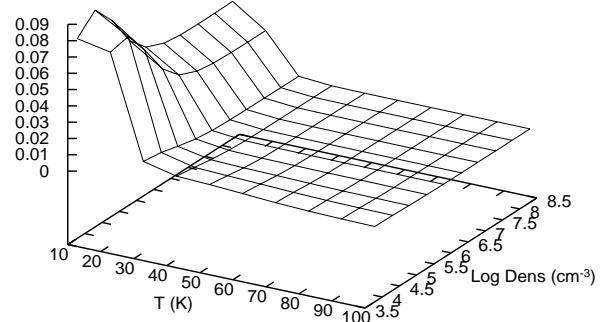


Fig. 3. Steady-state $[\text{DCO}^+]/[\text{HCO}^+]$ ratio, from our gas-phase model, varying with temperature and density

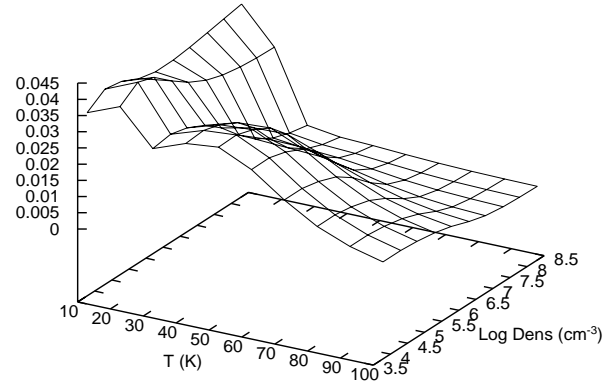


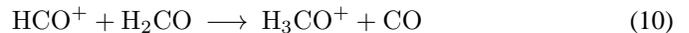
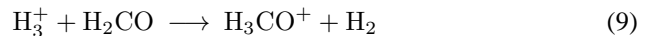
Fig. 4. Steady-state $[\text{DCO}]/[\text{HCO}]$ ratio, from our gas-phase model, varying with temperature and density

is a sharp rise in the fractionation of DCO^+ as the density falls. This is due to the reaction;



At low temperature and densities atomic deuterium is very abundant so reac. (8) proceeds very rapidly and can further enhance the fractionation of DCO^+ . However, as the density increases, $[\text{D}]$ decreases, and once $n(\text{H}_2)$ reaches a few times 10^5 cm^{-3} reac. (8) effectively switches off and the $[\text{DCO}^+]/[\text{HCO}^+]$ ratio drops.

Other species may be fractionated by different routes depending on the temperature and/or density. An example of this is DCO , illustrated in Fig. 4. Its hydrogenated analogue, HCO , is formed via the reactions;



followed by recombination of H_3CO^+ with electrons. Thus, in H_2DCO^+ the deuterium can either come from H_2D^+ , whose abundance is enhanced at 10 K, or from HDCO , whose abundance is enhanced at 50 K. At low densities, therefore, we get the double peaked temperature dependence of $[\text{DCO}]/[\text{HCO}]$ shown in Fig. 4.

For temperatures above $\sim 30 \text{ K}$ and H_2 densities above $\sim 10^5 \text{ cm}^{-3}$, the $[\text{DCO}]/[\text{HCO}]$ ratio is not significantly enhanced. The abundances of both HCO and DCO fall as the

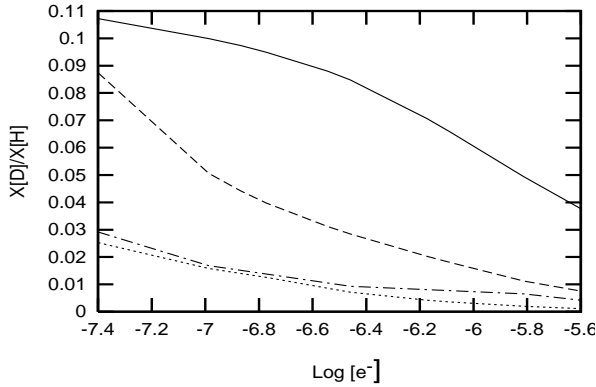


Fig. 5. The variation of selected molecular D/H ratios with fractional ionisation, from our gas-phase model at 10 K, $n(\text{H}_2) = 10^4 \text{ cm}^{-3}$, for $[\text{H}_2\text{D}^+]/[\text{H}_3^+]$ (solid), $[\text{DCO}^+]/[\text{HCO}^+]$ (dashed), $[\text{NH}_2\text{D}]/[\text{NH}_3]$ (dash-dot) and $[\text{DCN}]/[\text{HCN}]$ (dotted).

density increases (because they are formed via the dissociative recombination), but there is also a route to forming HCO via charge exchange between HCO^+ and iron atoms. This generally occurs so slowly that destruction of HCO^+ is dominated by electrons but, as $[e^-]$ falls, more HCO^+ can react with Fe. Once $n(\text{H}_2)$ reaches $\sim 10^5 \text{ cm}^{-3}$ this becomes the dominant formation route for HCO, whose abundance begins to rise. However, above $\sim 30 \text{ K}$ there is little enhancement of $[\text{DCO}^+]$ so it is not abundant enough to form significant amounts of DCO and $[\text{DCO}]$ continues to fall with increasing density. This analysis is supported by the fact that below 30 K, when $[\text{DCO}^+]/[\text{HCO}^+]$ is enhanced, the $[\text{DCO}]/[\text{HCO}]$ ratio does increase at high densities.

3.2. Dependence on fractional ionisation

Fractional ionisation is an important parameter in interstellar clouds, as it governs the interaction of the cloud material with the magnetic field and ultimately determines whether the cloud can support itself against gravitational collapse. The determination of the level of fractional ionisation is difficult because it is not directly observed. Instead, the most common approach is to use observations of deuterium fractionation, particularly via the $[\text{DCO}^+]/[\text{HCO}^+]$ ratio, combined with the use of Eq. (4), to derive limits (Williams et al. 1998). As a result, it is useful to have some indication how the molecular D/H ratios vary with ionisation.

Iron and silicon are included in our model as representative metals which influence the ionisation fraction of the system. To investigate the affect of this parameter on the deuterium fractionation we have varied the relative abundances of these metals between a few times 10^{-9} and a few times 10^{-6} , which has the affect of increasing the free electron abundance from $\sim 3 \times 10^{-8}$ to $\sim 5 \times 10^{-6}$.

In general, increasing the ionisation fraction decreases deuterium fractionation, because the electrons increasingly dissociate the primary ions before they can transfer their deuterium to other species. This is illustrated in Fig. 5. When $[e^-]$ is low

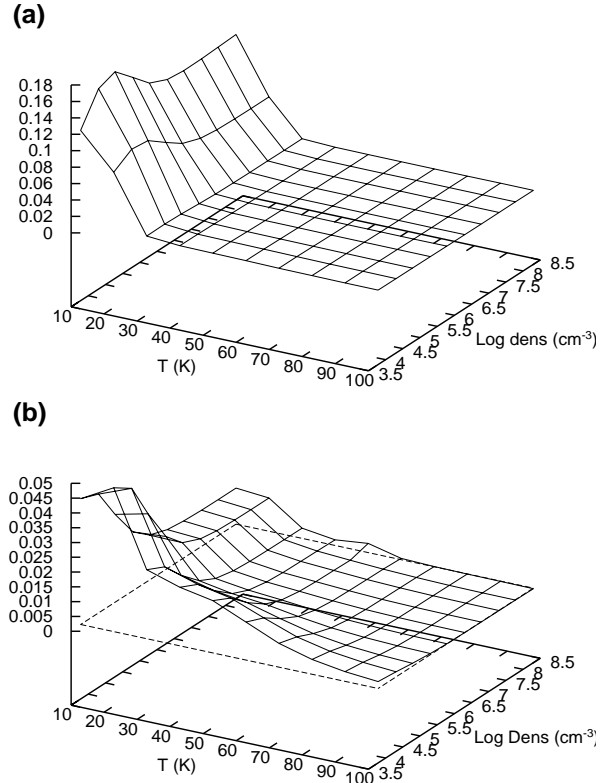


Fig. 6a and b. Steady-state $[\text{DCO}^+]/[\text{HCO}^+]$ ratio, from our gas-phase model using initial C, N and O abundances **a** three-times lower and **b** three times higher than listed in Table 2, varying with temperature and density. The dashed plane in **b** indicates the $[\text{DCO}^+]/[\text{HCO}^+]$ ratio observed towards the Galactic Centre.

(less than $\sim 10^{-7}$) the $[\text{H}_2\text{D}^+]/[\text{H}_3^+]$ ratio has only a weak dependence on $[e^-]$, and, in fact, tends towards a constant. For these low ionisation levels it is reactions with neutral species which determine the degree of fractionation. As the fractional ionisation increases, however, dissociative recombination of H_2D^+ becomes competitive with the neutral reactions and the $[\text{H}_2\text{D}^+]/[\text{H}_3^+]$ ratio decreases more sharply.

In a recent survey of around 20 sources Williams et al. (1998) found values for the ionisation fraction between $10^{-6.5}$ and $10^{-7.5}$. Comparing our theoretical values for fractionation of DCO^+ , NH_2D and DCN , from Fig. 5, with observations of these molecules in TMC-1 (Table 3) we can see that our model is in reasonable agreement at this level of ionisation.

3.3. Dependence on elemental abundances

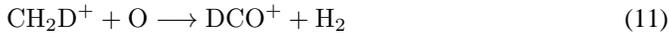
Increasing the relative abundances of elements such as C, N and O tends to decrease molecular D/H ratios in species fractionated by H_2D^+ , as we are increasing the importance of the third term in the denominator of Eq. (4). This can be seen by comparing Fig. 3 with Fig. 6, which shows the effect of altering C, N and O abundances on the $[\text{DCO}^+]/[\text{HCO}^+]$ ratio. At temperatures below 30 K fractionation drops with increasing elemental abundance, as we expect. At higher temperatures, however, the

Table 4. A Comparison of molecular D/H ratios observed in our local ISM with those observed towards the Large Magellanic Cloud (LMC) and towards the Galactic Centre (GC).

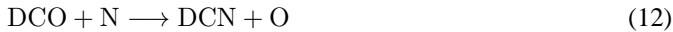
	Source	Temp. (K)	[DCO ⁺]/[HCO ⁺]	[DCN]/[HCN]	Refs.
LMC	N113	20–30	0.01–0.05	0.04	1
Local	TMC-1	10	0.02	0.023	2,3
	Orion	~70	0.002	0.003	4,5
GC	Sgr A	60–100	0.0002	0.0004	6,7

References: 1. Chin et al. 1996; 2. Tiné et al. 2000; 3. Wooten 1987; 4. Penzias 1979; 5. Schilke et al. 1992; 6. Jacq et al. 1999; 7. Lubowich et al. 2000

behaviour is more complex – at the point where $T_{\text{kin}} = 50$ K and $n(\text{H}_2) = 10^4 \text{ cm}^{-3}$ increasing the elemental abundances has increased the fractionation (from 0.004 in Fig. 3 to 0.015 in Fig. 6b). This is due to the formation of DCO⁺ via the reaction;



The energy barrier in reac. (2) means that the $[\text{CH}_2\text{D}^+]/[\text{CH}_3^+]$ ratio is enhanced up to ~60 K, while the increased oxygen abundance drives reac. (11) more efficiently. Fig. 7 shows that the $[\text{DCN}]/[\text{HCN}]$ ratio exhibits similar behaviour, its fractionation at certain temperatures and densities increasing with increasing elemental abundance. In this case, this is primarily due to the increasing importance of the reaction



as $[\text{N}]$ increases.

Heavy elements are made by nucleosynthesis in stars, a process which also destroys deuterium. The most active and heavily processed region of our galaxy is the Galactic Centre, where the high rate of star formation will have increased the metallicity and is expected to have destroyed much of the primordial deuterium. Conversely, the Magellanic Clouds are thought to be significantly less processed than our own Galaxy and may have lower elemental abundances and a higher underlying D/H ratio. Table 4 summarizes the observations of deuterium fractionation in these two regions and compares them with observations of our local ISM.

The primordial D/H ratio is an important cosmological parameter since it is related to the baryon density. However the current cosmic value, which is determined accurately only for the local interstellar medium, provides only a lower limit for the primordial value due to loss of deuterium in astration. The determination of the underlying D/H ratio in regions with different degrees of processing may tell us more about the astration processes and may put more stringent constraints on the primordial D/H ratio.

Although the underlying D/H ratio cannot easily be determined for very distant regions, emission from deuterated molecules has been observed throughout our Galaxy and in the Large Magellanic Cloud (LMC). We have attempted to use our model results to search for variations in the underlying D/H ratio as one moves away from the local ISM. The major problem

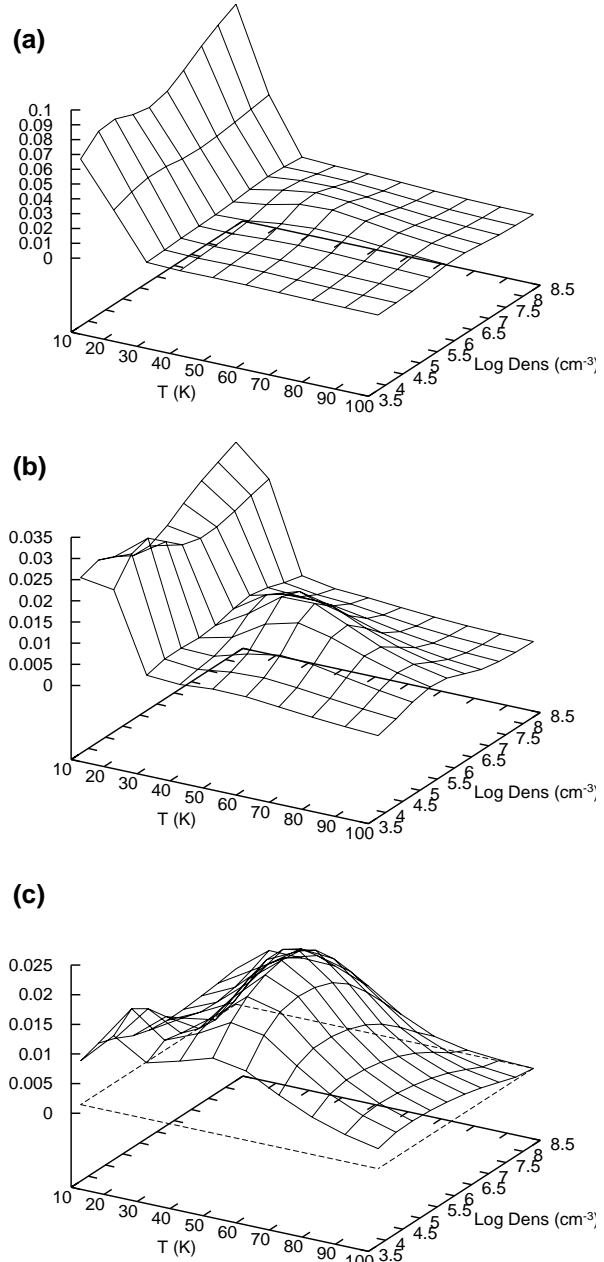


Fig. 7a–c. Steady-state $[\text{DCN}]/[\text{HCN}]$ ratio, from our gas-phase model using initial C, N and O abundances **a** three-times lower than, **b** equivalent to and **c** three times higher than those listed in Table 2, varying with temperature and density. The dashed plane in **c** indicates the $[\text{DCN}]/[\text{HCN}]$ ratio observed towards the Galactic Centre.

we face is that the physical parameters in clouds close to the Galactic Centre or in other galaxies are not known well enough to constrain D/H ratios which can be very sensitive, especially to temperature. However, we can still draw some general conclusions.

Fig. 7 shows the effects of altering initial elemental abundances on the $[\text{DCN}]/[\text{HCN}]$ ratio, over a wide range of physical conditions. To obtain a $[\text{DCN}]/[\text{HCN}]$ ratio as high as was observed towards the LMC we first need to consider a region with

Table 5. Comparison of abundances of sulphur-bearing molecules in TMC-1 (Ohishi & Kaifu 1998; upper limits from Walmsley 1993) with theoretical values from our gas-phase model at 10 K, $n(\text{H}_2) = 10^4 \text{ cm}^{-3}$.

Species	Observed abundance	Predicted abundance at steady state
CS	7.5(-09)	3.2(-08)
SO	4.0(-09)	1.2(-08)
H ₂ CS	9.0(-10)	1.1(-09)
HCS ⁺	5.0(-10)	2.2(-10)
H ₂ S	<5.0(-10)	1.1(-11)
SO ₂	<1.0(-09)	6.8(-09)

Note: a(-b) stands for $a \times 10^{-b}$

reduced metallicity (Fig. 7a). Assuming a cloud temperature of 20 K, the observations *are* consistent with the underlying D/H ratio we have assumed (i.e. $\sim 1.5 \times 10^{-5}$), but if temperatures were closer to 30 K the observations require a D/H ratio about 10 times larger. This result is consistent with the observations of DCO⁺ (compare Figs. 3 and 6a with the result in Table 4) and with the idea that the LMC is less processed than our own galaxy.

The molecular D/H ratios observed towards the Galactic Centre, on the other hand, are some ten times lower than those observed in our local ISM. Figs. 6b and 7c show that, even with increased elemental abundances, the Sgr A cloud would have to be extremely hot and dense to produce both the observed ratios. These constraints can be relaxed, however, if we assume that the underlying D/H ratio in this cloud has been reduced from that in the local ISM. A value of $\text{D}/\text{H} = 1.7 \times 10^{-6}$ is consistent with the observations of DCN and HCN in this cloud (Lubowich et al. 2000) and indicates a substantial degree of astration in this region.

4. Discussion

4.1. Sulphur chemistry

Fig. 8 shows the evolution of the abundances and fractionations of selected sulphur bearing species as predicted by our gas-phase model. At steady-state much of the sulphur is still in atomic form, with substantial amounts of the remainder in CS and SO. Table 5 shows that our predicted abundances are in good agreement with observations of TMC-1, but there is less observational data with which to compare our estimates of deuterium fractionation. Minowa et al. (1997) measured the $[\text{HDCS}]/[\text{H}_2\text{CS}]$ ratio in TMC-1 to be 0.02. Our model agrees with this result (to within a factor of two) and predicts a similar level of fractionation for other sulphur bearing, deuterated species.

When we now compare our predicted gas-phase abundances with those observed by van Dishoeck et al. (1995) in IRAS 16293 (a low-mass source, apparently a young binary system), the agreement is not so good. In one sense this is not surprising, since the observations are averages over an

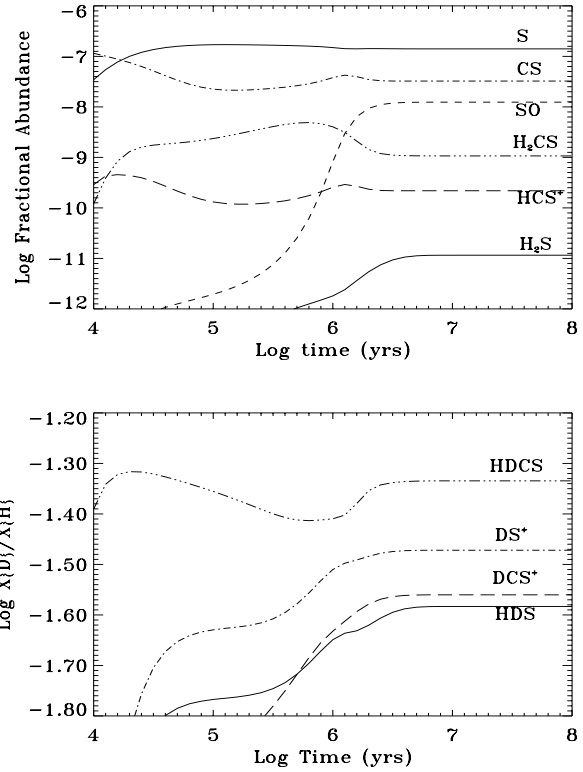
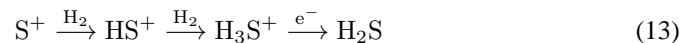


Fig. 8. The fractional abundances (top) and molecular D/H ratios (bottom), of selected sulphur-bearing species, varying over time, from our gas-phase model. $T_{\text{kin}} = 10 \text{ K}$, $n(\text{H}_2) = 10^4 \text{ cm}^{-3}$.

area which includes a hot, dense outflow region ($T_{\text{kin}} \geq 80 \text{ K}$; $n(\text{H}_2) \sim 10^7 \text{ cm}^{-3}$) as well as the cooler circumbinary envelope ($T_{\text{kin}} \sim 10\text{--}20 \text{ K}$; $n(\text{H}_2) \sim 10^4 \text{ cm}^{-3}$). However, van Dishoeck et al. measured the deuterium fractionation in some species (notably HDS and HDSCO) to be as high as 10%, a result which cannot be reproduced by our gas-phase chemistry, regardless of the temperature and/or density we assume. Such large ratios have, in the past, been used to argue that grain surface processes actively fractionate molecules.

Another possible explanation for this high fractionation is that accretion onto grains is occurring, thereby increasing the molecular D/H ratios, as discussed above. Using physical conditions similar to those found in the outer envelope of the binary system we have modeled the deuterium chemistry of an accreting cloud, which does indeed produce very high molecular D/H ratios for a time before everything freezes out (see Fig. 9). Fig. 9 also shows the predicted evolution of the relative abundances of some sulphur-bearing species. Table 6 shows how these modeled abundances compare with observations.

Although the agreement is generally good, there is one inconsistency – $[\text{H}_2\text{S}]$ is some ten times too low in our model. H_2S formation is a perennial problem for gas-phase chemistry. The main route to its formation is via the reaction chain;



but there is a large energy barrier to the reaction of S^+ with H_2 ($\sim 9860 \text{ K}$). At low temperatures S^+ can radiatively associate

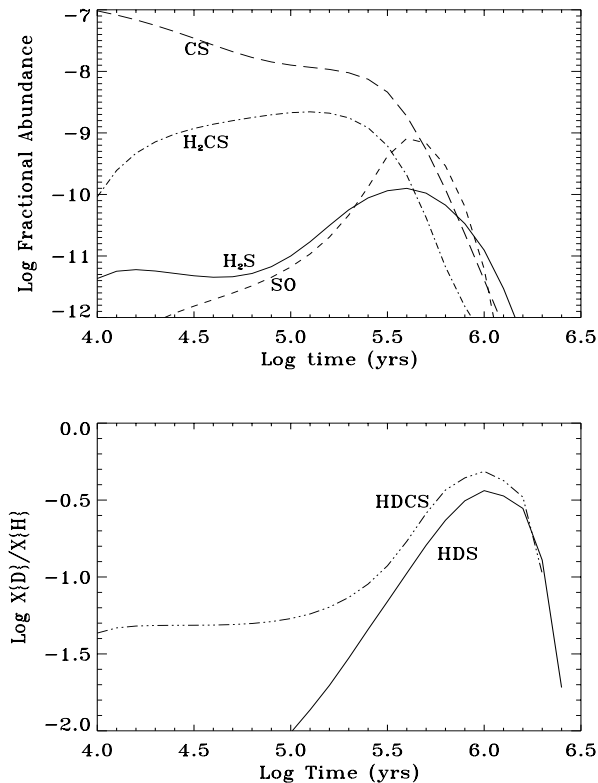


Fig. 9. The fractional abundances of selected species (top) and selected molecular D/H ratios (bottom), varying over time, from our depletion model. $T_{\text{kin}} = 10$ K, $n(\text{H}_2) = 10^4 \text{ cm}^{-3}$.

Table 6. Comparison of abundances of sulphur-bearing molecules in IRAS 16293 (van Dishoeek et al. 1995) with theoretical values from our depletion model at 10 K, $n(\text{H}_2) = 10^4 \text{ cm}^{-3}$.

Species	Observed abundance	Predicted abundance after 0.3 Myr
CS	1.1(-09)	4.6(-09)
SO	3.9(-09)	4.2(-09)
H ₂ CS	1.7(-10)	6.2(-10)
H ₂ S	1.5(-09)	1.1(-10)

Note: a(-b) stands for $a \times 10^{-b}$

with H₂ but the rate coefficient is very small (Herbst et al. 1989) so that H₂S and HDS do not form efficiently.

One explanation for the observed abundance is that we are seeing emission from the hot, shocked gas where the outflow from the young star interacts with the circumbinary envelope producing high enough temperatures to enhance H₂S production. However, deuterium fractionation is strongly dependent on temperature and we would not see such a large [HDS]/[H₂S] ratio if the temperature were much above 10 K. It seems more likely that, as in hot cores, which are generally associated with high-mass star formation, the HDS and H₂S are the products of grain-surface chemistry which have been returned to the gas-phase (Hatchell et al. 1999). A survey of deuterated species in other low-mass sources would be very useful, in order to see

whether these very high molecular D/H ratios are a general feature or particular to this source.

4.2. Doubly deuterated species

Gas-phase chemistry predicts that the ratio of any doubly deuterated species to its mono-deuterated analogue will be roughly the same as the ratio of the mono-deuterated species to its hydrogen-bearing analogue. Thus, for doubly deuterated species to be observable we require a high degree of fractionation in the mono-deuterated species.

Towards the Orion Compact Ridge Turner (1990) measured $[\text{HD}\text{CO}]/[\text{H}_2\text{CO}] \sim 0.14$, and $[\text{D}_2\text{CO}]/[\text{H}_2\text{CO}] \sim 0.003$. In this source the gas temperature should be high enough to preclude significant fractionation, so the enhanced molecular D/H ratios are usually thought to have been preserved, in grains mantles, from an earlier, colder phase. These particular ratios, however, cannot be reproduced from a standard gas-phase chemistry (see Fig. 10) and so imply that processing on the grain surfaces has further enhanced fractionation. This is supported by the more recent observations of Ceccarelli et al. (1998) and Loinard et al. (2000) towards IRAS 16293, who obtained even higher ratios ($[\text{HD}\text{CO}]/[\text{H}_2\text{CO}] = 0.13\text{--}0.16$, and $[\text{D}_2\text{CO}]/[\text{H}_2\text{CO}] = 0.05\text{--}0.06$).

As mentioned above, the detection of doubly deuterated species has been taken as an indicator of active grain surface chemistry followed by evaporation of the surface species back in to the gas. However, Roueff et al. (2000) have recently detected doubly deuterated ammonia (NHD₂) in the dark cloud L134N. The temperature in this region is thought to be < 10 K, too low for efficient evaporation of ice-mantles, and so these molecules are unlikely to be products of an active grain surface chemistry followed by desorption.

L134N was considered to be a good candidate for detecting NHD₂ because mono-deuterated species are so abundant there (e.g. $[\text{DCO}^+]/[\text{HCO}^+] = 0.18$; $[\text{NH}_2\text{D}]/[\text{NH}_3] = 0.1$). An alternative explanation for these very high molecular D/H ratios could be that they result from depletion onto grains. Fig. 10 shows the dramatic increase that occurs in the fractionation of both mono- and doubly deuterated species as freeze-out begins to be effective. It turns out that the $[\text{H}_2\text{D}^+]/[\text{H}_3^+]$ ratio is very sensitive to the abundances of heavier species, our models indicate that a 30% reduction of [CO] will enhance ratios such as $[\text{NH}_2\text{D}]/[\text{NH}_3]$, $[\text{DCO}^+]/[\text{HCO}^+]$ and $[\text{N}_2\text{D}^+]/[\text{N}_2\text{H}^+]$ to the levels observed in L134N.

Although doubly deuterated ammonia is not currently included in our model, these results are interesting in that the very large ratios of $[\text{HD}\text{CO}]/[\text{H}_2\text{CO}]$ and $[\text{D}_2\text{CO}]/[\text{H}_2\text{CO}]$ which are obtained after $\sim 10^6$ yrs also agree well with those observed in IRAS 16293. Thus, an *active* surface chemistry is not necessary to obtain very high fractionation.

4.3. Depletion in continuum clumps

Gas-phase species are expected to be depleted at the centres of cold, dark clouds, since they will tend to stick to the dust grains

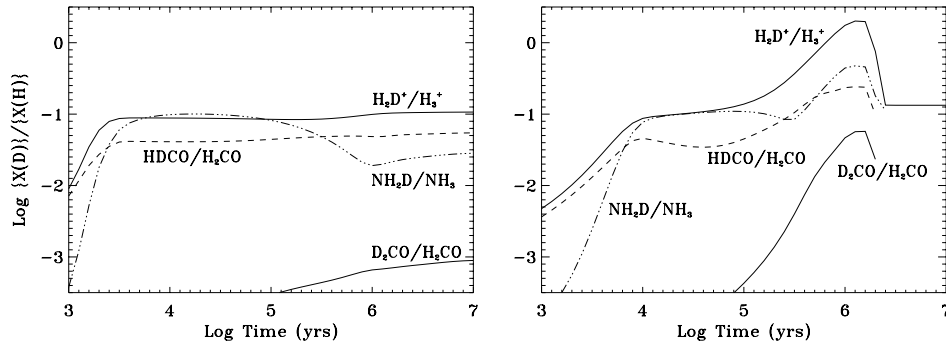


Fig. 10. A comparison of selected molecular D/H ratios predicted by our gas-phase (left) and depletion (right) models. $T_{\text{kin}} = 10$ K, $n(\text{H}_2) = 10^4 \text{ cm}^{-3}$.

they collide with. Gibb & Little (1998) have found that several dense clumps in Orion, identified by dust continuum emission and mapped in HCO^+ , are not apparent from mapping C^{18}O . They conclude that the CO abundance is reduced by a factor somewhere between 10 and 50, and believe that it has frozen onto the dust surfaces.

The very bright HCO^+ emission that they observed supports this interpretation, as it is most likely due to the removal of H_2O , a species which destroys HCO^+ . Our models do predict a slight increase in $[\text{HCO}^+]$ as depletion begins to set in (see Fig. 1), but this is dependent on the initial conditions we assume. However, we also see a much more pronounced increase in $[\text{DCO}^+]$ as CO and H_2O begin to freeze out, which is independent of initial conditions. Thus, measurements of molecular D/H ratios can be used as a more stringent test that depletion is taking place and also, alongside observations of other molecules, to test our chemical theories of the collapse phase.

Caselli et al. (1999) have observed DCO^+ and HCO^+ towards the starless cloud core L1544, where comparison between $[\text{C}^{17}\text{O}]$ and the dust emission indicates that CO is depleted by a factor of about ten. They estimate $[\text{DCO}^+]/[\text{HCO}^+] \sim 0.12$, six times higher than is seen in TMC-1.

We have modeled the variation of the $[\text{DCO}^+]/[\text{HCO}^+]$ ratio with temperature and density, using our depletion model. Fig. 11 shows that the ratio drops off sharply with temperature (as we expect from our gas-phase model), only exceeding 0.1 at temperatures below 20 K. Varying the density does not greatly affect the level of fractionation, however at high densities species freeze out much more quickly. As these enhancements are highly temperature dependant (especially in the range 10–20 K) a detailed thermal balance calculation is now required to investigate whether the removal of molecular coolants, such as CO, may affect the gas temperature and, hence, the fractionation.

5. Conclusions

We have used an updated, large, chemical kinetic model to explore the effects of parameter variation, including density, temperature, elemental abundances and grain accretion, on molecular D/H ratios. We find that the ratios vary widely with temperature, depending on the primary fractionation process. Thus ratios which are only affected by H_2D^+ chemistry (e.g. $[\text{N}_2\text{D}^+]/[\text{N}_2\text{H}^+]$, $[\text{DCO}^+]/[\text{HCO}^+]$) show a rapid fall-off once

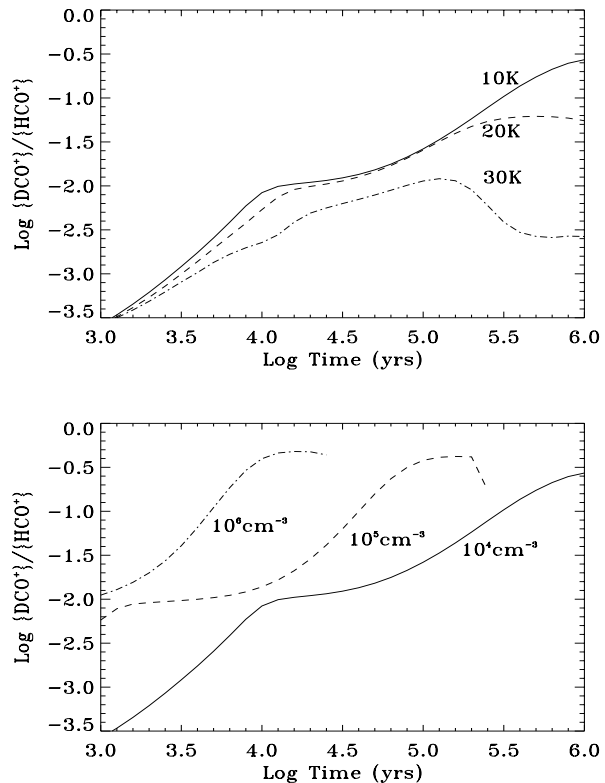


Fig. 11. The $[\text{DCO}^+]/[\text{HCO}^+]$ ratio varying with time, from our depletion model; *Top*: $n(\text{H}_2) = 10^4 \text{ cm}^{-3}$; *Bottom*: $T_{\text{kin}} = 10$ K.

the kinetic temperature is above 20 K. Other ratios in which the fractionation results from CH_2D^+ or C_2HD^+ remain large until 50–60 K.

Variations in the abundances of C, N and O affect the molecular D/H ratios such that, in general, increasing abundances correlate with decreasing fractionation, though at high temperatures (~ 50 K) some ratios can actually increase.

The chemical reaction scheme which has been developed for modelling local interstellar clouds can be applied to more distant regions of our galaxy, and even to other galaxies, where deuterium-bearing molecules have been observed. Although physical conditions and elemental abundances are not well determined for very distant regions we have been able to draw some general conclusions about the variation of the underlying D/H ratio which may help to constrain models of astration.

We have included the fractionation of sulphur-bearing molecules for the first time, finding good agreement with the very limited observational data in dark clouds. The very slow formation rates of H₂S and HDS in cold gas make these molecules particularly useful in probing regions where grain-surface chemistry may be important.

Molecular D/H ratios can become very large when material is allowed to accrete on to cold dust grains. In this case we find that gas-phase chemistry can give rise to very large abundances of both singly and doubly deuterated molecules. These large ratios do not require an active surface chemistry, contrary to previous expectations. A more rigorous calculation taking thermal balance into account is needed to see whether this result holds for all species.

Acknowledgements. HR is grateful to PPARC for the award of a studentship. Astrophysics at UMIST is supported by PPARC.

References

- Adams N.G., Smith D., 1985, *ApJ* 294, L63
 Bell M.B., Avery L.W., Matthews H.E., et al., 1988, *ApJ* 326, 924
 Caselli P., Walmsley C.M., Tafalla M., Dore L., Myers P.C., 1999, *ApJ* 523, L165
 Ceccarelli C., Castets A., Loinard L., Caux E., Tielens A.G.G.M., 1998, *A&A* 338, L43
 Chin Y.-N., Henkel C., Millar T.J., Whiteoak J.B., Mauersberger R., 1996, *A&A* 309, L33
 Crosswell K., Dalgarno A., 1985, *ApJ* 289, 618
 Gerin M., Combes F., Wlodarczak G., Encrenaz P., Laurent C., 1992, *A&A* 253, L29
 Gibb A.G., Little L.T., 1998, *MNRAS* 295, 299
 Guélin M., Langer W.D., Wilson R.W., 1982, *A&A* 107, 107
 Hatchell J., Roberts H., Millar T.J., 1999, *A&A* 346, 227
 Herbst E., Adams N.G., Smith D., DeFrees D.J., 1987, *ApJ* 312, 351
 Herbst E., DeFrees D.J., Koch W., 1989 *MNRAS* 237, 1057
 Howe D.A., Millar T.J., Schilke P., Walmsley C.M., 1994, *MNRAS* 267, 59
 Jacq T., Baudry A., Walmsley C.M., Caselli P., 1999, *A&A* 347, 957
 Larsson M., Lepp S., Dalgarno A., et al., 1996, *A&A* 309, L1
 Linsky J.L., Diplas A., Wood B.E., et al., 1995, *ApJ* 451, 335
 Loinard L., Castets A., Ceccarelli C., et al., 2000, *A&A* 359, 1169
 Lubowich D.A., Pasachoff J.M., Balonek T.A., et al., 2000, *Nat* 405, 1025
 MacLeod J.M., Avery L.W., Broten N.W., 1981, *ApJ* 251, L33
 Millar T.J., Bennett A., Herbst E., 1989, *ApJ* 340, 906
 Millar T.J., Farquhar P.R.A., Willacy K., 1997, *A&AS* 121, 139
 Minowa H., Satake M., Hirota T., et al., 1997, *ApJ* 491, L63
 Ohishi M., Kaifu N., 1998, *Faraday Dis.* 109, 205
 Penzias A.A., 1979, *ApJ* 228, 430
 Rodgers S.D., Millar T.J., 1996, *MNRAS* 280, 1046
 Roueff E., Tiné S., Coudert L.H., et al., 2000, *A&A* 354, L63
 Sidhu K.S., Miller S., Tennyson J., 1992, *A&A* 255, 453
 Schilke P., Walmsley C.M., Pineau des Forets G., et al., 1992, *A&A* 256, 595
 Smith D., Adams N.G., Alge E., 1982a, *ApJ* 263, 123
 Smith D., Adams N.G., Alge E., 1982b, *J. Chem. Phys.* 77, 1261
 Sundström G., Mowat J.R., Danared H., et al., 1994, *Sci* 263, 785
 Tiné S., Roueff E., Falgarone E., Gerin M., Pineau des Forêts G., 2000, *A&A* 356, 1039
 Turner B.E., 1989, *ApJ* 347, L39
 Turner B.E., 1990, *ApJ* 362, L29
 van Dishoek E.F., Blake G.A., Jansen D.J., Groesbeck T.D., 1995, *ApJ* 447, 760
 Walmsley C.M., 1993, *J. Chem. Soc. Faraday Trans.* 89, 2119
 Watson W.D., 1976, *Rev. Mod. Phys.* 48, 513
 Willacy K., Millar T.J., 1998, *MNRAS* 298, 562
 Williams J.P., Bergin E.A., Caselli P., Myers P.C., Plume R., 1998, *ApJ* 503, 689
 Wooten A., 1987, In: Vardya M.S., Tarafdar S.P. (eds.) *Astrochemistry*. Reidel, Dordrecht, p. 311